# Effectively Intervening Epithelial-Mesenchymal Transition of Retinal Pigment Epithelial Cells With a Combination of ROCK and TGF-β Signaling Inhibitors

Yi Chen,[1,2] Binxin Wu,[1,2] Jian Feng He,[3] Jingyao Chen,[1] Zi Wei Kang,[1] Dandan Liu,[1] Junjie Luo,[1] Kexin Fang,[1] Xiaoxu Leng,[1] Haibin Tian,[1,2] Jingying Xu,[1,2] Caixia Jin,[1,2] Jieping Zhang,[1,2] Juan Wang,[1,2] Jingfa Zhang,[1,2] Qingjian Ou,[1,2] Lixia Lu,[1,2] Furong Gao,[1,2] and Guo-Tong Xu[1,2]

[1]Department of Ophthalmology of Shanghai Tenth People's Hospital, and Tongji Eye Institute, and Department of Pharmacology, Tongji University School of Medicine, Shanghai, China
[2]Department of Biochemistry and Molecular Biology, Tongji University School of Medicine, Shanghai, China
[3]Department of Biochemistry and Molecular Cell Biology, Shanghai Key Laboratory of Tumor Microenvironment and Inflammation, Shanghai Jiao Tong University School of Medicine, Shanghai, China

**PURPOSE.** Epithelial-mesenchymal transition (EMT) of retinal pigment epithelial (RPE) cells is a key pathological event in proliferative retinal diseases such as proliferative vitreoretinopathy (PVR). This study aimed to explore a new method to reverse EMT in RPE cells to develop an improved therapy for proliferative retinal diseases.

**METHODS.** In vitro, human embryonic stem cell–derived RPE cells were passaged and cultured at low density for an extended period of time to establish an EMT model. At different stages of EMT after treatment with known molecules or combinations of molecules, the morphology was examined, transepithelial electrical resistance (TER) was measured, and expression of RPE- and EMT-related genes were examined with RT-PCR, Western blotting, and immunofluorescence. In vivo, a rat model of EMT in RPE cells was established via subretinal injection of dispase. Retinal function was examined by electroretinography (ERG), and retinal morphology was examined.

**RESULTS.** EMT of RPE cells was effectively induced by prolonged low-density culture. After EMT occurred, only the combination of the Rho-associated coiled-coil containing protein kinase (ROCK) inhibitor Y27632 and the TGF-β receptor inhibitor RepSox (RY treatment) effectively suppressed and reversed the EMT process, even in cells in an intermediate state of EMT. In dispase-treated Sprague-Dawley rats, RY treatment maintained the morphology of RPE cells and the retina and preserved retinal function.

**CONCLUSIONS.** RY treatment might promote mesenchymal-epithelial transition (MET), the inverse process of EMT, to maintain the epithelial-like morphology and function of RPE cells. This combined RY therapy could be a new strategy for treating proliferative retinal diseases, especially those involving EMT of RPE cells.

Keywords: EMT, RPE, TGF-β, ROCK, PVR

Retinal pigment epithelial (RPE) cells are monolayer cells located between the neural retina and the choroid and play essential roles in the maintenance of neuroretinal survival and function.[1] Usually, RPE cells are quiescent and rarely divide throughout life. However, when RPE cells are damaged by the destructive effects of different endogenous or exogenous factors, they re-enter the cell cycle and proliferate. Such proliferation in lower vertebrates, such as newts, results in neuroretinal regeneration.[2,3] In contrast, in higher vertebrates, such as rodents and humans, RPE proliferation is generally accompanied by pathological epithelial-mesenchymal transformation (EMT), loss of

epithelial phenotype and function, and adoption of a fibroblastic phenotype with increased proliferation and migration activity, eventually leading to severe retinal diseases, such as proliferative vitreoretinopathy (PVR).[4–7] Over the years, a great deal of research has been performed to treat such retinal diseases, but the results have been far from satisfactory. Prevention of EMT in RPE cells may be a promising therapeutic strategy for the treatment of these diseases, and an effective way to repress EMT in RPE cells deserves intensive study.

EMT plays a vital role in tissue healing and organ fibrosis. The development of EMT in RPE cells is a process similar to the damage repair response,[8] involving the combined action of multiple signaling pathways, such as the transforming growth factor–beta (TGF-$\beta$) and Rho-associated coiled coil-forming protein kinase (ROCK) signaling pathways. In addition, loss of cell-cell contact was found to initiate EMT and proliferation in RPE cells.[9] Although TGF-$\beta$ is a potent inducer of EMT, it cannot effectively induce EMT in RPE cells with intact cell-cell adhesion.[9,10] Furthermore, it is more challenging to induce confluent epithelial cells to undergo EMT via TGF-$\beta$ pathway activation than subconfluent cells with few contacts.[10–13] Therefore, disruption of cell-cell adhesion is necessary for EMT to occur, and other EMT inducers mainly accelerate the EMT process.

Numerous drugs have demonstrated efficacy in inhibiting EMT in vitro. However, the effects of these molecules in vivo is not evident. For example, Src inhibitors were reported to inhibit EMT,[14,15] yet their clinical effects were disappointing.[16,17] This may be due to the difference between the EMT states of the cells in vivo and in vitro. When potential drugs are tested in clinical trials, RPE cells in patients might have already begun EMT, and patient RPE cells may even be in a later stage of the EMT process. In contrast, the interventions to suppress EMT in in vitro studies were usually given before or at the same time as EMT induction, when the EMT process had just begun or was in an early stage,[18–21] which allowed mesenchymal-epithelial transition (MET) to occur readily. In other words, the EMT inhibitors developed in preclinical studies could only prevent EMT and could not reverse EMT that had already occurred in patients.

To develop a robust strategy that addresses the issue mentioned above, we sought to identify small molecules that reverse late-stage EMT in RPE cells. Using a low-density-induced EMT model, we found that the combination of RepSox, a TGF-$\beta$ inhibitor, and Y27632, a ROCK inhibitor, effectively reversed EMT in RPE cells, even after RPE cells were cultured at low density for six days. Furthermore, the combination of these two molecules effectively reduced the subretinal dispase-induced EMT in rat RPE cells, as demonstrated by the improved visual function, the well-maintained morphology of the retina and RPE, and the decreased $\alpha$-Smooth muscle actin ($\alpha$-SMA) expression in RPE cells.

## MATERIAL AND METHODS

### Derivation and Maintenance of hES-RPE Cells

The SHhES2 human embryonic stem cell (hESC) line was a generous gift from Professor Y. Jin (Institute of Health Sciences, Chinese Academy of Sciences, Shanghai, China) and was cultured on irradiated mouse embryonic fibroblasts in ESC medium (Dulbecco's modified Eagle's medium: nutrient mixture F-12 [DMEM/F-12; Gibco, Thermo Fisher Scientific, Waltham, MA, USA] ) supplemented with

0.1 mM 2-mercaptoethanol [Gibco], 0.1 mM minimum essential medium nonessential amino acids [MEM NEAA; Gibco], 2 mM L-glutamine [Gibco], 1% penicillin-streptomycin [Gibco], 20% knockout serum replacement [KSR; Gibco], and 4 ng/mL BFGF [R&D Systems, Minneapolis, MN, USA]) in a humidified atmosphere of 5% $CO_2$ at 37°C. The medium was changed every two days.

For RPE cell differentiation, SHhES2 cells were dissociated into clumps by treatment with collagenase IV and then plated on 1% Matrigel-coated dishes for an hour. The attached cell aggregates were covered with 2% Matrigel diluted in neural differentiation medium consisting of DMEM/F-12 and neurobasal medium (1:1) supplemented with 1% N2 and 1% B27 (Gibco). After 24 hours of incubation, the cells were cultured for five days with neural differentiation medium that was changed every other day. Then the cells were cultured for 30 to 35 days with hESC medium containing 10% KSR (10% KSR medium). Pigmented patches were collected with collagenase IV and plated on 1% Matrigel-coated 6-well plates in 10% KSR medium with 10 mM nicotinamide (Sigma-Aldrich Corp., St. Louis, MO, USA). The medium was changed every two to three days. The RPE cells derived from SHhES2 cells (hES-RPE cells) used in experiments were between passages three and five.

**The hES-RPE Confluence.** The cells were grown in six-well tissue plates coated with 1% Matrigel (Corning Inc., Corning, NY, USA). For 50% confluency, $1.5 \times 10^6$ cells were seeded into each well. For 25%, 12.5%, 8%, 6.25%, and 3.125% confluence, the number of cells seeded was calculated in proportion to that for 50% confluence.

**Cell Culture in Transwells.** The hES-RPE cells were plated in Transwells (Corning Inc.) coated with 1% Matrigel. The seeded cell number was calculated in proportion to that of cells on 6-well plates.

For small molecule treatment, the cells were first incubated in 10% KSR medium for different days before being given fresh media containing various small molecules (10 µM RepSox and/or 10 µM Y27632; Selleck Chemicals, Houston, TX, USA) and cultured for 14 days.

### Animals

Six-week-old Sprague-Dawley (S-D) rats were supplied by SLACCAS (Shanghai, China) and maintained in the Tongji University Animal Center. All animals used in this study were maintained in specific pathogen-free conditions in microisolator cages and were treated in accordance with the guidelines provided in the ARVO statement for the Use of Animals in Ophthalmic and Vision Research and the Guides for the Care and Use of Animals (National Research Council and Tongji University).

### Subretinal Injection of RepSox and Y27632 Into the Experimental Rats

The protocol was approved by the Committee on the Ethics of Animal Experiments of Tongji University (Permit Number: TJAA09620204). In vivo RPE-EMT models with PVR-like conditions were established as previously reported[22] with modifications. Briefly, after anesthetization with 2% sodium pentobarbital, S-D rats were administered 3 µL of 1 µg/µL dispase (Gibco) via subretinal injection. A channel was created by inserting a 30-gauge needle behind the limbus into the vitreous chamber. Then, a 33-gauge needle was

inserted into the subretinal space through the vitreous chamber, and a 3 μL mixture was injected into the area near the center of the retina. The eyes that received the same volume of PBS were used as controls, and dimethyl sulfoxide (DMSO) was used as the vehicle control. One and three weeks after the injection, the rats were examined for ERG responses and then euthanized, and RPE-Bruch's membrane choriocapillaris complexes were isolated for use in assays as described previously.[23]

### Vibratome Sectioning

To visualize cross sections of the Transwells, vibratome sectioning was performed as described previously[24] with slight modifications. Briefly, after two weeks of culture, RPE cells on Transwells were fixed with 4% PFA for 10 minutes and 1% glutaraldehyde for 30 minutes. Then, the Transwell inserts were split with a razor blade into small fragments and embedded in 10% low melting agarose (Sangon Biotech, Shanghai, China). The embedded RPE cells were cut into 150 μm sections at medium speed and amplitude in a vibratome (Leica, Wetzlar, Germany). The sections were used for 4′,6-diamidino-2-phenylindole (DAPI) staining on glass slides.

### Low Calcium Culture

The hES-RPE cells were collected and washed twice with PBS and then cultured at 50% confluency in calcium-free keratinocyte SFM (KSFM; Gibco). The cells were divided into two groups. The low $Ca^{2+}$ group was cultured in KSFM supplemented with 2 μM $Ca^{2+}$, and the normal $Ca^{2+}$ group was cultured in KSFM supplemented with 1 mM $Ca^{2+}$. After seven days, the medium of the low $Ca^{2+}$ group was replaced with normal $Ca^{2+}$ KSFM. Both groups of cells were cultured for seven more days and then collected for examination.

### Transepithelial Electrical Resistance (TER) Measurement

TER was measured with a Millicell-ERS2 Volt-Ohm Meter (Millipore, Burlington, MA, USA) 14 days after cell plating. As previously described,[25] the short electrode was immersed in the upper compartment, and the long electrode was immersed in the bottom compartment. The final TER value ($\Omega \cdot cm^2$) was calculated by the following formula: TER = ($TER_{sample} - TER_{blank}$) × the surface area of the Transwell.

### EdU Proliferation Assay

The hES-RPE cells were cultured at 12.5% confluency in 12-well tissue plates and treated with RepSox and Y27632 for three days. Then, the cell proliferation assay was conducted with an EdU Cell Proliferation Kit (Beyotime Institute of Biotechnology, Jiangsu, China). The cells were incubated with 5-ethynyl-2′-deoxyuridine (EdU, 10 μM) for two hours. The EdU-incorporating cells (S phase) were analyzed following the manufacturer's instructions. Briefly, the isolated cells were fixed and permeabilized with 4% PFA and 0.3% Triton X-100 (Sigma-Aldrich Corp.). Then, the cells were stained with Click Reaction Buffer (Azide Alexa Fluor 488; ThermoFisher, St. Louis, MO, USA). Propidium iodide was added to each sample immediately before flow cytometry analysis (CytoFLEX LX Flow Cytometer; Beckman Coulter, Inc, South-field, MI, USA). The results were analyzed by FlowJo 7.6 and are expressed as percentages of cells in each phase of the cell cycle and were calculated from the mean ± SD of three independently replicated experiments.

### Cell Scratch Assay

When hES-RPE cells grew to 100% confluence in six-well tissue plates, the cells were washed twice with sterile PBS. The cell monolayer in each well was then scratched with a sterile plastic tip, and the cells were washed twice with PBS and incubated in KSR-free medium in the presence of RepSox, Y27632 or both for 48 hours. The cells and wound were imaged at 0, 24, and 48 hours, and the area of wound closure was calculated with ImageJ 1.46r software (National Institutes of Health) for three independent replicate experiments.

### Scotopic Flash Electroretinogram (fERG) Examination

After the small molecules were injected into the subretinal space, ERG a-wave and b-wave amplitudes were measured weekly up to 12 weeks after surgery with an AVES-2000 electrophysiological apparatus (Chongqing Kanghua Ruiming S&T Co., Ltd, Chongqing, China) as described previously.[26,27] An intensity of $6.325 \times e^{-2} cd*s/m^2$ was applied to record the response of photoreceptors to light stimulation (n = 8 eyes in each group).

### Preparation of Retinal Cryosections

Rats were euthanized at weeks 1 and 3. The eyeballs were removed immediately and fixed in 4% PFA. The embedded tissues were sectioned (10 μm thickness, 36 slices for each eye) along the vertical meridian of the eyeball, and the cryosections that crossed the optic disc were used for analysis. To assess the distortion of the retina, the nuclei in the sectioned tissue were stained with DAPI.

### Immunostaining

For immunofluorescence analysis, hES-RPE cells cultured in Transwells or in 24-well culture plates were fixed with 4% (vol/vol) PFA in PBS for 10 minutes, permeabilized with 0.25% Triton X-100 (Sigma-Aldrich Corp.) for five minutes, washed with PBS, and then blocked with 3% BSA (Sangon Biotech) in PBS. The sections were incubated with primary antibodies against ZO-1, $\alpha$-SMA, F-Actin, and PAI-1 overnight at 4°C. They were then washed three times with PBS, followed by incubation with the fluorescent secondary antibodies for one hour. DAPI was used to visualize the nuclei. Samples from three independent experiments were examined with a fluorescence microscope (Olympus IX73; Olympus, Tokyo, Japan). The primary antibodies used are listed in Supplementary Table S1.

### Western Blot Analysis

Total proteins from cells were extracted on ice in RIPA Lysis Buffer (Beyotime Institute of Biotechnology) containing protease and phosphatase inhibitor cocktails (Bimake, Houston, TX, USA), followed by centrifugation at 12,000 rpm and 4°C for 20 minutes. The protein concentration of the

supernatant was determined by BCA assay (Pierce, Appleton, WI, USA). In total, 15 to 30 μg of the protein lysate was loaded on a 7% to 15% polyacrylamide gel and transferred to a polyvinylidene fluoride membrane (Millipore). The blots were blocked with 5% milk or 5% BSA in TBS +0.1% Tween 20 and incubated with primary antibodies against Zeb1, ZO-1, FN1, PAI-1, $\alpha$-SMA N-Cadherin, E-Cadherin, DCT, CRALBP, OTX2, MITF, ACTB, RPE65, Smad2/3, Phospho-Smad2/3, and GAPDH in 5% BSA overnight at 4°C. This step was followed by incubation with the corresponding HRP-conjugated secondary antibodies (Proteintech, Rosemont, IL, USA) for one hour at room temperature. Visualization of proteins was performed by using Thermo ECL Western Blotting Detection Reagent and Gel (Thermo Fisher Scientific). The blots were then reprobed with GAPDH or $\beta$-actin antibody. Densitometric analysis of proteins was performed by Tanon 5200S (Bio-Equip, Nanjing, China). The data are representative of three independent experiments. The primary antibodies used are listed in Supplementary Table S1.

## Quantitative Real-Time RT-PCR (qRT-PCR) Detection

Total RNA was extracted from cells using TRIzol reagent (Takara Bio, Kyoto, Japan) according to the manufacturer's instructions. The concentration of RNA was measured with a Nanodrop 2000 spectrophotometer (Thermo Fisher Scientific), and cDNA was synthesized from 1 μg of total RNA using a reverse transcription kit (Takara Bio). Specific primers were used to detect stem/RPE/EMT-related RNA expression, with GAPDH used as an internal control. RNA quantification was performed using the BioRad CFX96TM Real-Time PCR Detection System. The relative amount of each gene was calculated using the $2^{-\Delta\Delta CT}$ method. All qRT-PCR experiments were performed in triplicate. The primer sequences are listed in Supplementary Table S2.

## Statistical Analysis

The statistical software package GraphPad Prism version 6.0 (GraphPad Software, San Diego, CA, USA) was used to analyze the data. Statistical testing involved a two-tailed Student's *t*-test or two-way ANOVA with Tukey's multiple comparison test as appropriate. Data are expressed as the mean ± SEM or SD, as indicated.

## RESULTS

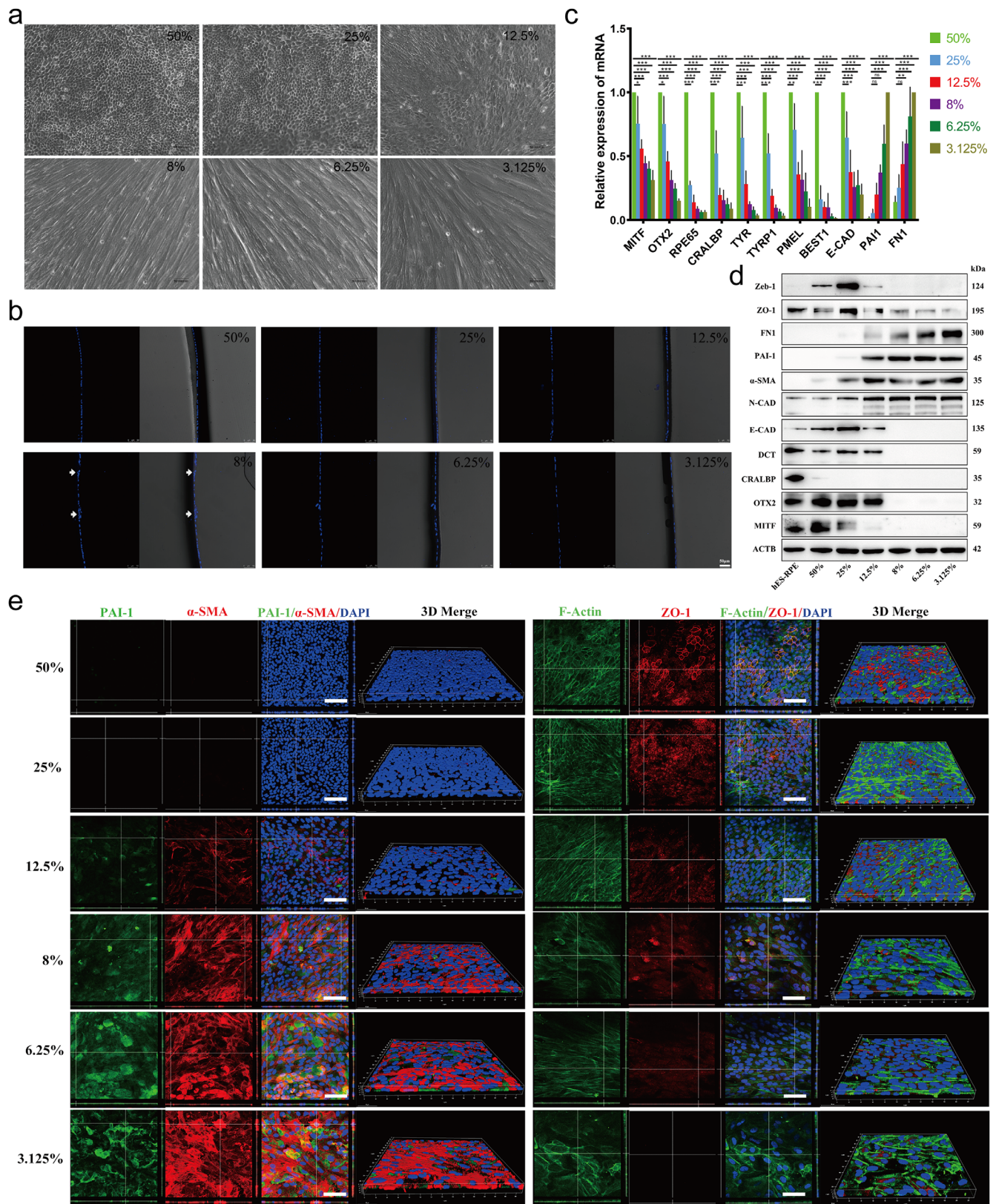### EMT of RPE Cells is Activated in a Cell Density- and Time-Dependent Manner

RPE cells were reported to undergo EMT readily with repeated passage or in low-density culture conditions.[21,28] To further clarify the relationship between cell culture density and EMT occurrence in RPE cells, minimally passaged hESC-derived RPE cells were cultured at different confluences (from 3.125% to 50%) for 14 days. As shown in Figure 1a, the RPE cells maintained epithelial morphology at 25% to 50% confluence but rapidly developed mesenchymal morphology at cell confluences of 3.125% to 12.5%. Vibratome sections of RPE cells grown in Transwells showed that RPE cells grew in a monolayer but occasionally aggregated in low-density cultured cells (Fig. 1b, white arrow), suggesting that RPE cells in low-density culture could form

fibrous nodules. The TER of RPE cells cultured in Transwells increased gradually with increasing cell density in culture (Supplementary Fig. S1). As expected, RPE cells cultured at 50% confluency had a higher TER value than RPE cells cultured at lower densities.

Furthermore, both quantitative PCR (Q-PCR) and Western blot analyses confirmed the downregulation of RPE-related genes, such as MITF, OTX2, RPE65, CRALBP, TYR, TYRP1, PMEL, Best and E-Cadherin, and the upregulation of EMT-associated genes, such as PAI-1, FN1, and $\alpha$-SMA, with decreasing cell confluence (Figs. 1c and 1d). Figure 1e shows the immunofluorescence staining of a tight junction protein (ZO-1), phalloidin (F-actin), and EMT markers ($\alpha$-SMA and PAI-1) in the cultured cells at different densities. It was clear that when cultivated at 50% confluence, the cells exhibited a tightly connected hexagonal morphology, with ZO-1 and F-actin localized along the cell boundary. In contrast, the cells cultured at 25% confluence and below showed fewer or no tight junctions between the cells, accompanied by increased stress fibers and sharply increased $\alpha$-SMA and PAI-1 expression. These results confirmed that the EMT process in RPE cells was activated by low-density culture and that the level of EMT depended on cell confluence. Therefore 3% and 12.5% confluence was used for the experiments in this study. We also examined the cell morphology and expression of RPE and EMT markers in cells cultured at higher density (60% and 80% confluency). There was little difference in the morphology of RPE cells cultured at 80%, 60% and 50% confluency (Supplementary Fig. S2a). Although the expression levels of some RPE markers, such as MITF, at 80% confluency were higher than those at 50% confluency, there were no significant differences in the expression levels of other RPE markers or EMT markers (Supplementary Figs. S2b and S2c). Therefore we used 50% confluency as the normal RPE culture condition in this study.

In addition, the results above also indicated that cell junctions might be a critical factor in initiating the EMT process. Thus we studied whether the absence of cell junctions could induce EMT. RPE cells were cultured at 50% confluency in normal (1 mM) and low Ca²⁺ (2 μM) KSFM. At three days, the control cells (normal Ca²⁺) had spread on the substrate and had an epithelial morphology, whereas the experimental cells (low Ca²⁺) showed a less adherent pattern and had a fusiform morphology (Supplementary Fig. S3a). After switching to normal Ca²⁺ media for seven days (14 days after the initial plating), the low Ca²⁺-cultured cells exhibited mesenchymal morphology (Supplementary Fig. S3a). Q-PCR analysis supported the morphological results (Supplementary Figs. S3b and S3c), indicating that loss of cell junctions induced EMT, consistent with a previous report that disruption of cadherin ligation by EGTA initiated EMT in RPE cells.[11]

To test whether the cell culture time was also involved in the activation of EMT, RPE cells were cultured at 12.5% and 50% confluence for different durations. Along with the extension of culture time, the cells cultured at 50% confluence gradually formed epithelial morphology. In contrast, 12.5% confluent cells gradually became spindle shaped and showed a fibrotic tendency (Fig. 2a). Q-PCR analysis showed that there was no obvious difference in the expression levels of RPE- or EMT-related markers among the cells cultured at 50% confluence for different durations (Fig. 2b). However, for the cells cultured at 12.5% confluence, the expression of RPE markers decreased, whereas that of EMT-related genes increased gradually with prolonged culture time (Fig. 2c),

**FIGURE 1.** EMT of RPE cells is activated in a cell density–dependent manner. **(a)** Representative images showing the different morphologies (cobblestone-like or disordered) of RPE cells cultured at 3.125%, 6.25%, 12.5%, 25%, and 50% confluence for 14 days. *Scale bar:* 50 μm. **(b)** Vibratome sections of RPE cells grown in Transwells for 14 days were stained with DAPI to show the nuclei in the RPE monolayer. DAPI-stained images were taken with a confocal microscope. *White arrow*: cell aggregation. *Scale bar:* 50 μm. **(c)** The mRNA expression levels of the RPE markers MITF, OTX2, RPE65, CRALBP, TYR, TYRP1, PMEL, BEST, and E-Cadherin and the EMT markers PAI-1 and FN1 were tested by RT-PCR in RPE cells cultured at different confluences for 14 days. Data are presented as the means ± SEM (n = 3 per group with duplicates). All data were normalized to the expression of each gene at 50% confluence except for those of PAI-1 and FN1 at 3.125%

confluence. *$P < 0.05$, ** $P < 0.01$ and ***$P < 0.001$ versus the 50% group. **(d)** The protein levels of RPE- and EMT-related genes in RPE cells cultured at different confluences for 14 days were examined by Western blot assays. RPE cells cultured at 50% confluence for four weeks were used as the mature RPE control. The results are representative of at least three independent experiments. **(e)** RPE cells cultured in Transwells at different confluences for 14 days were examined by immunofluorescence staining to demonstrate the localization of PAI-1, $\alpha$-SMA, F-actin, and ZO-1 in the cells. The orthogonal view and three-dimensional view were obtained using a confocal microscope. Left, *Green:* PAI-1; *Red:* $\alpha$-SMA; DAPI: nuclei. Right, *Green:* F-actin; *Red:* ZO-1; DAPI: nuclei. *Scale bar*: 50 µm.
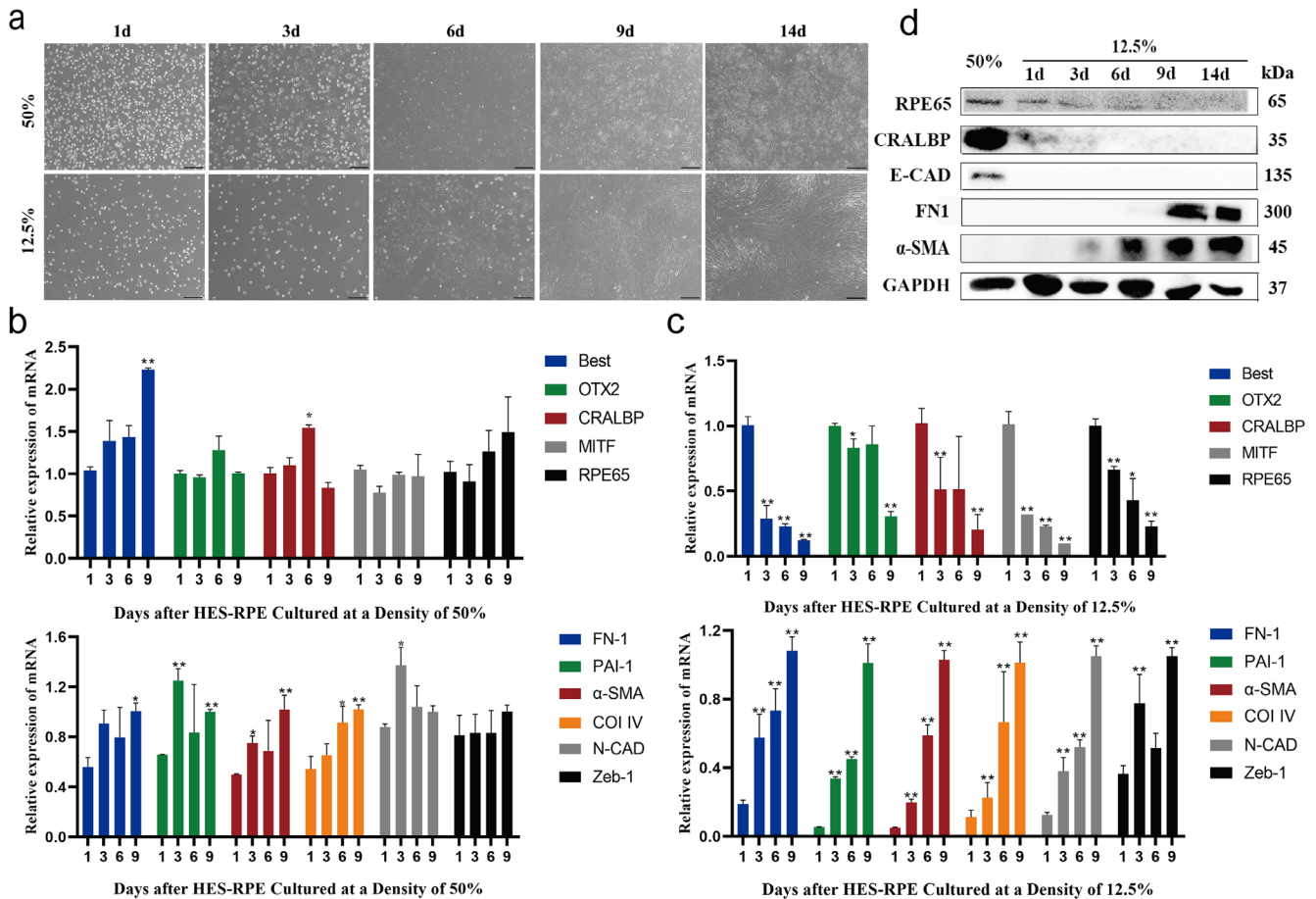


**FIGURE 2.** EMT of RPE is activated in culture time-dependent manner. **(a)** Representative images of RPE cells cultured at 50% and 12.5% confluence for one, three, six, nine, and 14 days. *Scale bar*: 100 µm. **(b–c)** The mRNA expression levels of the RPE markers OTX2, MITF, RPE65, Best, CRALBP, and PMEL and the EMT markers FN1, PAI-1, $\alpha$-SMA, Col IV, Zeb-1, and N-Cadherin were tested by RT-PCR in RPE cells cultured at 50% **(b)** and 12.5% **(c)** confluence for one, three, six, and nine days (n = 3 per group with duplicates). *$P < 0.05$, **$P < 0.01$ versus the one-day group. Data were normalized to GAPDH. **(d)** Western blotting bands showing the expression of RPE65, CRALBP, E-Cadherin, FN1, and $\alpha$-SMA in RPE cells cultured at 12.5% confluence for one, three, six, nine, and 14 days. RPE cells cultured at 50% confluence for 14 days were used as the mature RPE control. The results are representative of at least three independent experiments.

indicating that EMT of hES-RPE cells was facilitated by low-density culture. These observations were also confirmed by Western blot examination (Fig. 2d).

These data indicated that both reduction of the cell confluence in culture and extension of the culture time activated the EMT process. There is probably a gradient of EMT levels (ranging from no EMT to partial EMT and then full EMT) corresponding to the reduction of cell density or the extension of culture time. For the convenience of subsequent statements, we arbitrarily defined cells cultured for one day as cells in the "early" stage of EMT, those cultured for three to seven days as cells in the "middle" stage of EMT, and those cultured for nine days as cells in the "late" stage of EMT.

## Combined Treatment With RepSox and Y27632 Induces Differentiation and Inhibited EMT of RPE Cells in Vitro

Given the existence of an EMT gradient in low-density cultured RPE cells, our next challenge was to determine at which stage the EMT process could be reversed and whether such a reversal could be accomplished by the known EMT inhibitor Y27632, which is a specific inhibitor of the ROCK/RHO family of protein kinases.[29–34] To answer these questions, hES-RPE cells were plated at 12.5% confluence to induce EMT, and Y27632 was added at different times after cell plating. The cells were then cultured until 14 days after plating, and the cell morphology was
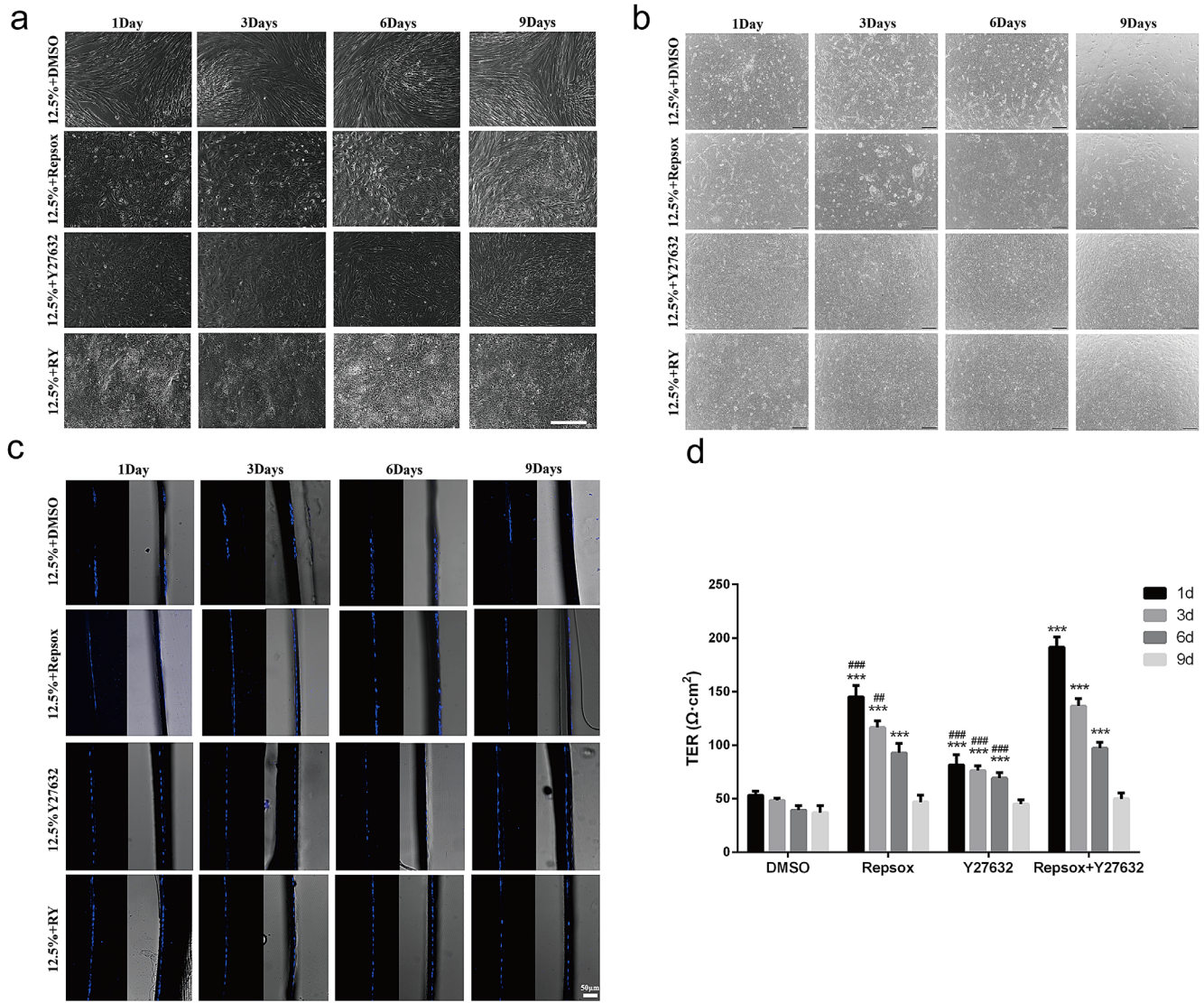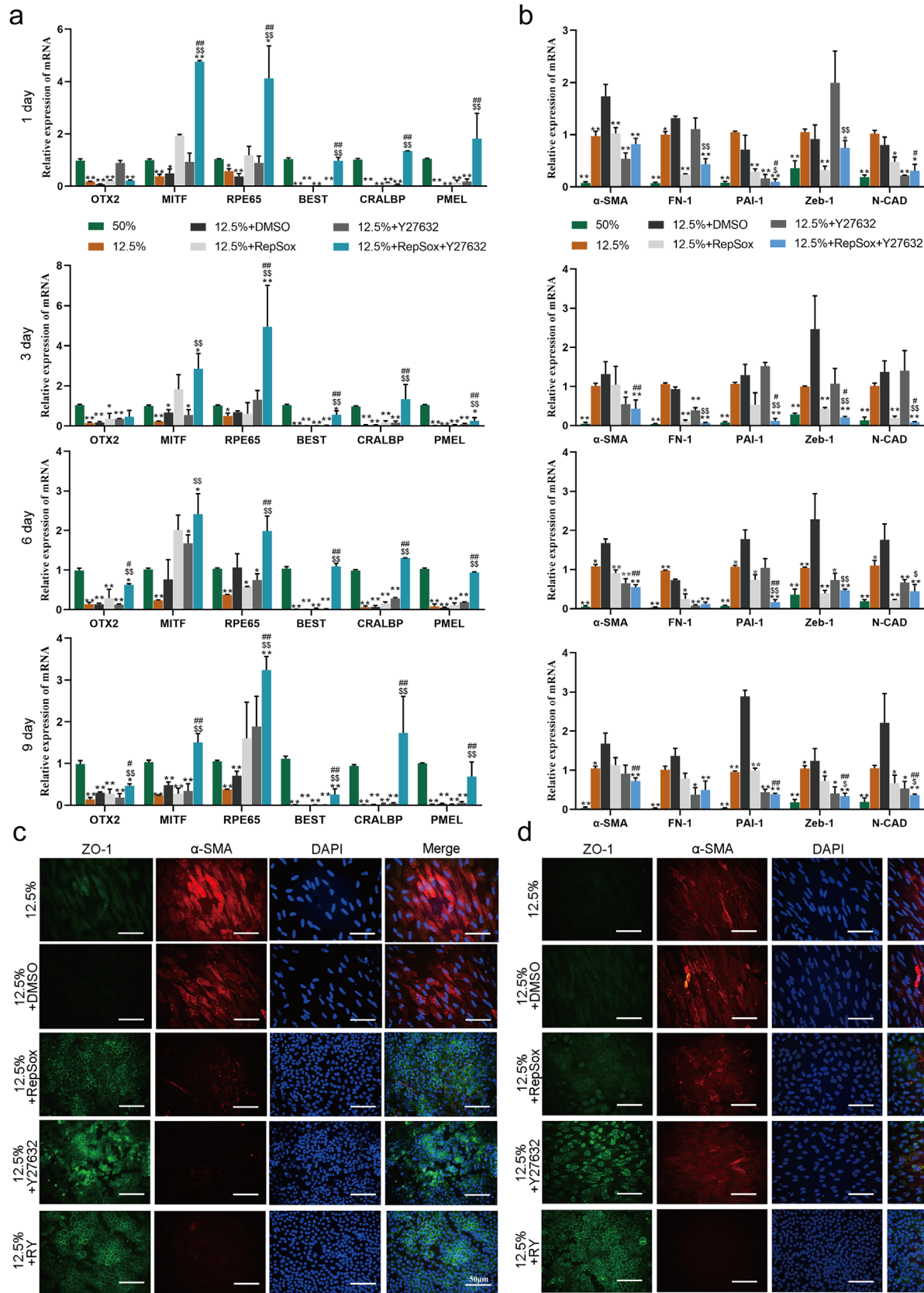
**FIGURE 3.** The combination of RepSox and Y27632 inhibits EMT of RPE cells in vitro. **(a–b)** Representative images of RPE cells cultured at 12.5% confluence on plates (**a**, *Scale bar*: 50 μm) and Transwells (**b**, *Scale bar*: 100 μm) for 14 days with small molecules added at different days as indicated. **(c)** Vibratome sections of RPE cells grown in Transwells for 14 days were stained with DAPI to show the nuclei in the RPE monolayer. *Scale bar*: 50 μm. **(d)** TER levels of RPE monolayers with small molecules added on different days as indicated. The TER levels were detected with a Millicell-ERS2 Volt-Ohm Meter at 14 days after cell plating. **\*\****P* < 0.001 versus the DMSO group. **##***P* < 0.01 and **###***P* < 0.001 versus the RepSox+Y27632 group.

examined. As shown in Figure 3a, Y27632 showed the ability to maintain RPE epithelial morphology only when it was added to the culture during the early stage of EMT, namely, at one day after cell plating, but not when it was added at three days or later. Compared with the RPE cells treated with Y27632 during the early stage, the RPE cells treated on day 3 or later showed significantly decreased expression of RPE-related genes (Fig. 4a) and increased expression of EMT-related genes (Fig. 4b).

Furthermore, to identify a condition under which middle- or even late-stage EMT is reversed, we screened a collection of reported molecules individually and in combination with Y27632 under low-density EMT-inducing conditions. RPE cells were cultured at 3.125% confluence for three and seven days and then maintained in medium supplemented with Y27632 and different molecules to modulate RPE cell proliferation and differentiation for an additional 14 days (Supple-

mentary Figs. S4a and S4b). We found that nicotinamide, PD0325901 (an ERK signaling inhibitor), RepSox (a TGF-$\beta$ signaling inhibitor), or epidermal growth factor (EGF), in combination with Y27632, demonstrated positive effects in maintaining RPE-like morphology to varying degrees when given on the third day after plating. Among these treatments, only the combination of RepSox and Y27632 (RY treatment) effectively prevented the loss of RPE morphology when given on the seventh day after plating.

In addition to morphological changes, the effects of these drug combinations on RPE- and EMT-related gene expression were also evaluated (Supplementary Figs. S4c and S4d). In general, the effects of the treatments on gene expression reflected the morphological observations. The cells treated with nicotinamide, PD032590, RepSox or EGF in the presence of Y27632 showed much lower expression of EMT marker genes and higher levels of RPE marker

**FIGURE 4.** The combination of RepSox and Y27632 inhibits the EMT of RPE cells in vitro. **(a–b)** The expression of RPE markers **(b)** and EMT markers **(c)** was tested by RT-PCR in RPE cells cultured at 12.5% confluence for 14 days with small molecules added to the culture on the first, third, sixth, and ninth days after plating (n = 3 per group with duplicates). The expression level of each gene relative to its expression level in the 50% group (for RPE markers) or the 12.5%+DMSO group (for EMT markers), which was set at 1, is shown. *$P < 0.05$, **$P < 0.01$,

versus the 12.5% + DMSO group. [#]$P < 0.05$, [##]$P < 0.01$, versus the 12.5%+RepSox group. [$]$P < 0.05$, [$$]$P < 0.01$, versus the 12.5%+Y27632 group. Data were normalized to GAPDH. **(c–d)** Immunofluorescence staining showed the localization of ZO-1 and the expression of $\alpha$-SMA in RPE cells cultured at 12.5% confluence for 14 days with the indicated molecules added to the culture on days 3 **(a)** and 6 **(b)** after plating. *Green*: ZO-1; *Red*: $\alpha$-SMA; DAPI: nuclei. *Scale bar*: 50 µm.

genes when these molecules were added on the third day in culture (Supplementary Fig. S4c). Interestingly, although all four combinations inhibited the expression of EMT markers when added on the seventh day, only RY treatment resulted in significantly increased expression of mature RPE markers (RPE65, CRALBP, and Best) (Supplementary Figs. S4c and S4d), supporting the observation that RY treatment not only inhibited EMT but also promoted RPE differentiation.

The above promising data encouraged us next to explore whether RepSox also has a positive effect on cultured RPE cells and how strong such a rescue effect would be. As shown in Figure 3, RepSox only inhibited the early stage of EMT and did not reverse the middle or late stage of EMT. However, when RepSox was combined with Y27632, the treatment effectively reversed the middle stage and even the late stage of EMT (Fig. 3a). We also cultured RPE cells in Transwells under different conditions and obtained similar results: RY treatment reversed low-density–induced EMT (Fig. 3b). All RPE cells treated with RY grew as a monolayer (Fig. 3c). Furthermore, the RY-treated RPE cells exhibited a stronger barrier property and lower permeability, as indicated by the higher TER value, than those treated with Y27632 or RepSox alone (Fig. 3d).

Additionally, compared with treatment with Y27632 or RepSox alone, treatment with a combination of both molecules significantly increased the expression of RPE-related genes and decreased the expression of EMT-related genes (Fig. 4a and 4b). The significantly enhanced effects of RY treatment were also supported by immunological examination, which revealed evident suppression of $\alpha$-SMA expression and good preservation of ZO-1 localization on the cell membrane, whereas separate treatment with either RepSox or Y27632 was less effective (Fig. 4c and 4d).

## The Combined Treatment of RepSox and Y27632 Promotes Proliferation and Inhibited Migration of RPE Cells
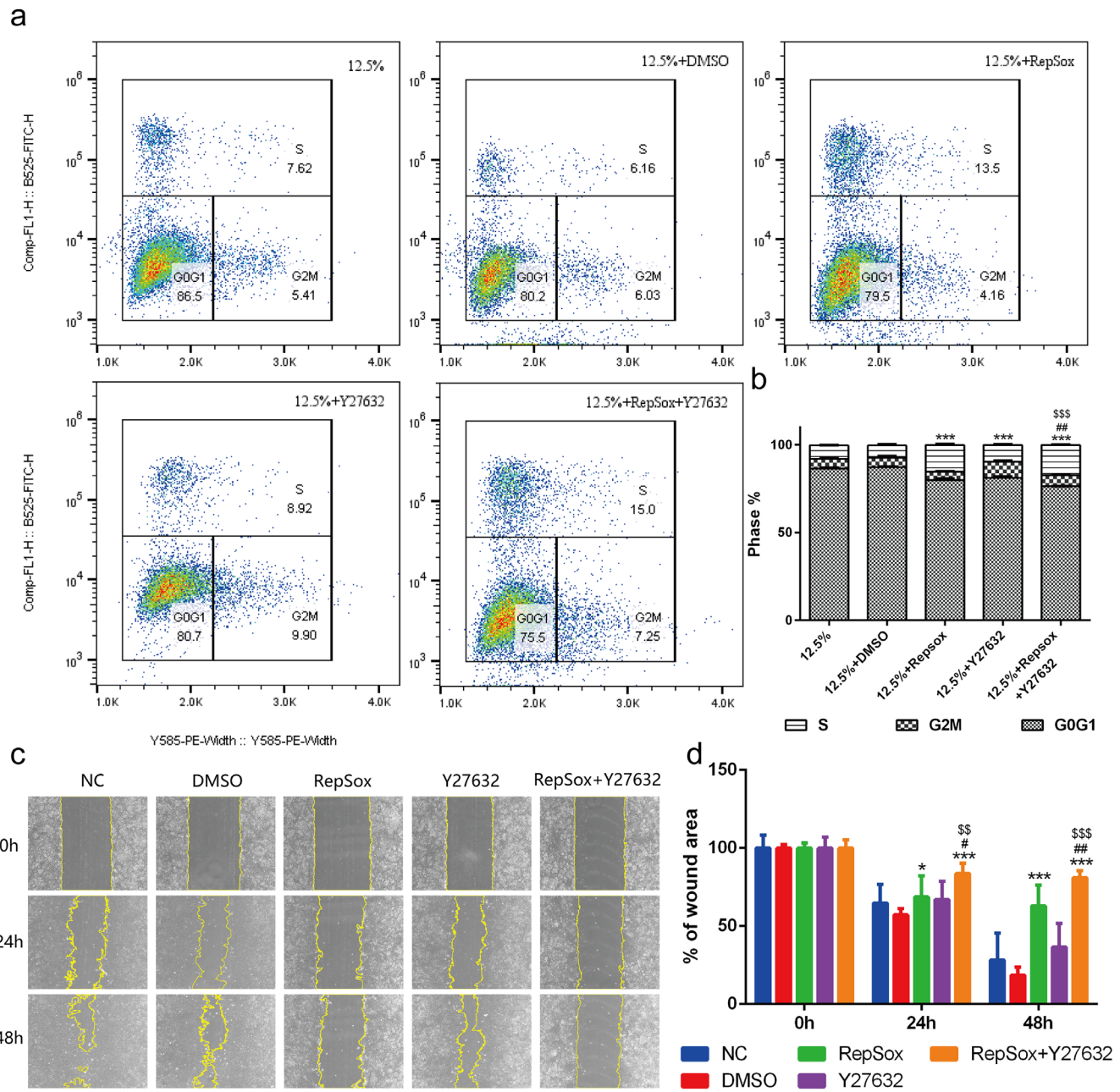
Because proliferation and migration are two of the most critical characteristics of EMT, we performed an EdU incorporation assay and wound healing assay to examine the influences of RepSox, independently or in combination with Y27632, on the proliferation and motile activity of hES-RPE cells. As shown in Figures 5a and 5b, at 12.5% confluence, all the treatments evidently increased the percentages of hES-RPE cells in S phase to different levels in comparison with the control group. These data indicated that either RepSox or Y27632 could promote the proliferation of RPE cells. In addition, the wound healing assay showed that the migration of hES-RPE cells was attenuated by RepSox during the experimental period ($P < 0.01$, vs. the DMSO group), whereas Y27632 showed no effect on RPE cell migration (Figs. 5c and 5d). These results demonstrated that either RepSox or Y27632 could promote RPE cell proliferation and RepSox inhibited cell migration and such effects could be significantly enhanced when they were used together (RY treatment), stronger than the simple addition of the effects of each of the two compounds.

## Combined Treatment With RepSox and Y27632 Inhibits EMT in RPE Cells and Protects Retinal Function in Vivo

To verify that the observed inhibitory effects of RepSox or Y27632 on EMT of cultured RPE cells also occur in vivo, a rat model of a PVR-like condition was established via administration of dispase, a nonspecific neutral metalloproteinase that impairs cell-cell interaction, following a similar method described in previous reports.[22,35] First, we assessed the damage to the visual function of the model rats and the protective effect of the treatments. The S-D rats were subretinally injected with dispase, and their visual function was examined with ERG at different time points. As shown in Figures 6a and 6b, at one week after injection, the amplitudes of both the a and b waves in the dispase injection group (a wave: $17.84 \pm 2.33$ µV; b wave: $57.62 \pm 8.86$ µV) were significantly lower than those in the PBS injection group (a wave: $38.80 \pm 5.85$ µV, $P < 0.001$; b wave: $152.42 \pm 14.02$ µV, $P < 0.001$). There was no significant difference between the untreated group and the PBS injection group at any time point. More excitingly, the intervention of the combined treatment of RepSox and Y27632 successfully reversed the dispase-induced reduction in visual function, and this effect lasted for at least 12 weeks (Figs. 6a and 6b). Notably, the effect of RepSox or Y27632 alone was much weaker and lasted for only one week, indicating that neither RepSox nor Y27632 was sufficient to maintain the visual function of the dispase-induced model and that combined therapy was necessary to achieve this effect.

Then, we examined the histology of the eyes of these rats to investigate the pathological basis of visual loss and the effect of RY treatment. As shown in Figures 6c and 6d, at one and three weeks after injection, only one to five layers of photoreceptors remained in the outer nuclear layer (ONL) of the dispase-treated rats, but RY treatment preserved the retinal ONL, and eight to 10 layers of photoreceptors were clearly observed. Furthermore, flat-mounted RPE samples were examined for tight junctions and EMT by immunostaining with antibodies against ZO-1 and $\alpha$-SMA. As shown in Figure 6e, compared with the PBS control group, the dispase group showed a disrupted pattern of ZO-1 expression and increased expression of $\alpha$-SMA at one week after injection. At three weeks after injection, both RPE injury and $\alpha$-SMA expression increased, suggesting that more severe damage to the RPE occurred with time. RY treatment maintained the regular membrane-associated localization pattern of ZO-1 and the normal level of $\alpha$-SMA expression.

These in vivo data indicated that subretinal dispase injection successfully induced a rat model that mimicked the effects of PVR both functionally and morphologically, including vision loss as well as RPE damage and EMT. The data also demonstrated that the combined treatment of RepSox and Y27632 effectively rescued visual function and photoreceptors by preventing EMT activation in the RPE and preserving cell-cell junctions, even though these two molecules showed little effect when each of them was used independently.
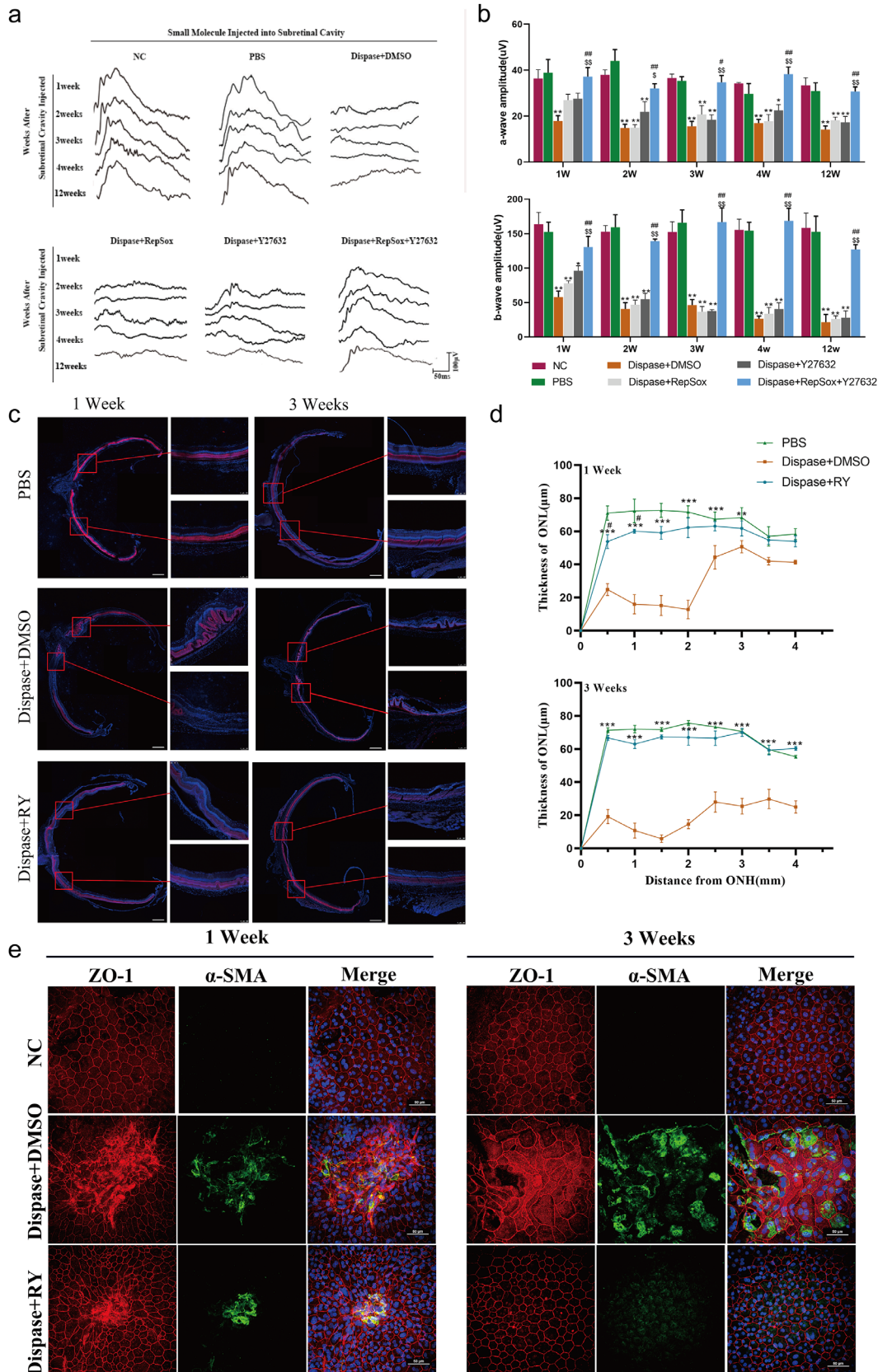
**FIGURE 5.** The effects of the combination of RepSox and Y27632 on the proliferation and migration of RPE cells. **(a)** Representative density dot plots showing the EdU incorporation of RPE cells in the five groups by FACS. **(b)** The percentages of RPE cells in different phases of the cell cycle after 72 hours of culture (n = 3 per group with duplicates). ***$P < 0.001$ versus the 12.5%+DMSO group. #$P < 0.01$ versus the 12.5%+RepSox group. $$$$$P < 0.001$ versus the 12.5%+Y27632 group. The results are from at least three independent experiments. **(c)** Representative images showing wound closure of RPE cells at zero, 24, and 48 hours after scratching. *Scale bar*: 100 μm. **(d)** Statistical analysis of the percentages of wound area of RPE cells at zero, 24, 48 hours after scratching (n = 9 per group with duplicates). There were three images from each experiment, and at least three independent experiments were performed. *$P < 0.05$, ***$P < 0.001$ versus the DMSO group. #$P < 0.05$, ##$P < 0.01$ versus the 12.5%+RepSox group. $$$$P < 0.01$, $$$$$P < 0.001$ versus the 12.5%+Y27632 group.

## DISCUSSION

During the investigation of the mechanisms of proliferative retinal diseases such as PVR, EMT of RPE cells was found to be an important pathological change. Subsequent studies focused on EMT regulatory signaling pathways and molecules. Among them, TGF-β signaling plays a vital role in EMT activation, and inhibition of the TGF-β pathway dramatically reduces the passage-dependent loss of epithe-lial potential.[23] However, TGF-β itself was unable to initiate EMT in RPE cells with intact cell junctions, although it accelerated the EMT process in cells that had already undergone EMT.[9] Disruption of cell junctions among RPE cells was the first step in their EMT, and this initial change activated Wnt signaling and inactivated the Hippo pathway, promoted the expression of EMT-related transcription factors and repressed the expression of RPE genes such as MITF and Otx2.[4] These studies mainly focused on the

**FIGURE 6.** The combination of RepSox and Y27632 inhibits EMT of RPE cells and maintains visual function in vivo. **(a)** Representative fERG waves of the normal control (NC), PBS treatment (PBS), dispase plus DMSO treatment (dispase+DMSO), dispase plus RepSox treatment (dispase+RepSox), dispase plus Y27632 treatment (dispase+Y27632), and dispase plus RepSox combined with Y27632 treatment (dispase+RepSox+Y27632) groups at 1, 2, 3, 4, and 12 weeks after injection (PI) were measured by scotopic flash electroretinography (fERG) at a flash intensity of $6.325 \times e^{-2}$cd*s/m$^2$. **(b)** Statistical analysis of the amplitudes of fERG a-waves

and b-waves at $6.325 \times e^{-2}$cd*s/m$^2$ in the six groups at one, two, three, four, and 12 weeks PI (n = 8 eyes per group). *$P < 0.05$, **$P < 0.01$ versus the PBS group. $^\#P < 0.05$, $^{\#\#} P < 0.01$ versus the dispase+RepSox group. $^\$P < 0.05$, $^{\$\$}P < 0.01$ versus the dispase+Y27632 group. (c) Representative images of whole retinal sections (*scale bar*: 500 μm) that crossed the optic disc were cola- beled with the photoreceptor marker recoverin (*red*) and DAPI (*blue*). The areas adjacent to the optic disc were collected to show the relative thickness of the outer nuclear layer (ONL) in the three groups at one and three weeks PI. *Scale bar*: 100 μm. (d) Measurement of the thickness of the ONL in the retinas of S-D rats in the PBS, dispase+DMSO and dispase+RepSox+Y27632 groups at one and three weeks PI (n ≥ 4 eyes per group). ONH: optic nerve head. **$P < 0.01$, ***$P < 0.001$ versus the dispase + DMSO group. $^\#P < 0.05$ versus the PBS group. (e) RPE-Bruch's membrane choriocapillaris complex images showing the cobblestone-like morphology of RPE cells from the dispase + RepSox + Y27632 group and the disordered appearance of RPE cells from the dispase + DMSO group at one and three weeks PI. RPE cells from the PBS group were used as normal controls. *Red*: ZO-1; *Green*: α-SMA; DAPI: nuclei. *Scale bar*: 50 μm.

---

inhibition of TGF-$\beta$–induced EMT to exclude the effects of other signaling pathways related to EMT of RPE. In the present study, we used a new approach, disruption of cell-cell connections, to create EMT models both in vitro and in vivo. In these two systems, we studied the initiation of EMT and the inhibitory effects of some molecules on EMT to establish new models for related studies, to clarify the possible mechanism and to find a more effective therapy for retinal diseases involving EMT of RPE cells.

In the low cell density–induced EMT model, we found that the EMT level depended on cell confluence (Fig. 1). However, it was unexpected that Zeb1 expression decreased at low confluency. Considering that lower cell density corre- lates with more advanced EMT we propose two possible explanations. As a transcription factor, Zeb1 is important and required for EMT in the early stage but may not be neces- sary in the late stage. Another possible explanation is the senescence of the cells in the low-density culture. It was reported that senescence was associated with the develop- ment of EMT,[36] and Zeb1 expression decreased in cells with ultraviolet A-induced senescence.[37]

EMT, a transition between the epithelial state and mesenchymal state,[38] is made up of a series of states called intermediate or partial EMT states between the two endpoints,[20] and the whole process is regulated by vari- ous signaling pathways and molecules. For RPE cells, when cultured at high plating density and low passage, the cells were maintained in a partial EMT status, and they could be reverted to the RPE state under proper conditions. In previ- ous reports, EMT inhibitors were added to RPE culture either before or at the same time as EMT induction,[19,21,30] and their effects can be claimed to prevent the cells from undergo- ing EMT but not to reverse it. In the present study, to test the ability of some known molecules to reverse the EMT process, the ROCK inhibitor Y27632, nine other molecules, or combinations of each of them with Y27632 were adminis- tered after EMT started, that is, they were added to cultured RPE cells after the occurrence of EMT. When Y27632 was tested alone, it restored the epithelial morphology of RPE cells cultured at low density for one day (cells in an early stage of EMT) but showed no effect on cells cultured for 3 or more days (cells in an intermediate EMT stage) (Fig. 3a). The main changes in the RPE cells cultured at low density for 3 or more days included significantly decreased expression of RPE-related genes and increased expression of EMT-related genes (Figs. 2b and 2c) compared with the cells cultured for one day. This result suggested that prolonged low-density culture led to the middle or late intermediate states of EMT, and by those states, some changes in gene transcription and protein translation had already occurred; thus Y27632 addi- tion at these intermediate states did not reverse EMT since it targets signaling molecules involved in an earlier stage of EMT.

In addition to Y27632, 4 other molecules tested in this study (nicotinamide, PD0325901, RepSox and EGF) also showed some effects in early EMT stages and might also regulate the signaling pathways related to early changes in the EMT process. However, when these 4 molecules were separately combined with Y27632 and tested in the low-density and longer culture-induced EMT model, we obtained the exciting result that treatment with a combination of RepSox and Y27632 (RY treatment) effectively reversed the EMT of RPE cells. In previous reports, TGF-$\beta$ induced cell cycle arrest,[39,40] and ROCK inhibition promoted the prolifer- ation of RPE cells.[29,41] Consistent with these results, RepSox and Y27632 were found to promote RPE cell proliferation, and their combination showed a more significant positive effect on RPE cell proliferation (Fig. 5a). Furthermore, RY treatment was examined for its effect on RPE cell migra- tion, another primary characteristic of EMT, in an in vitro scratch model. However, in contrast to previous reports that Y27632 promoted the migration of RPE cells in wound heal- ing assays,[41,42] Y27632 did not enhance RPE cell migration (Fig. 5b) in this study, suggesting that cell culture conditions might affect the response to Y27632. In contrast, RepSox alone showed significant inhibition of RPE cell migration, and this inhibitory effect was further strengthened when RepSox was combined with Y27632 (Fig. 5b). Regarding the possible mechanism of RY treatment, we believe it involves the superimposition of the effects of RepSox and Y27632. RepSox was reported to promote cell prolifera- tion[43] and lead to EMT-MET through its reprogramming role,[44,45] whereas Y27632 strengthened cell-cell adhesion, cell attachment, and cell junctions but had little effect on proliferation. When RepSox and Y27632 were used together, they promoted the reestablishment of cell-cell connections and adhesion, which are favorable for cell polarity and the MET process. This hypothesis could also explain the find- ing in one of our recent reports that RY added to cultured mouse RPE cells inhibited the EMT of the cells and main- tained their epithelial-like morphology.[45] Another possible mechanism is related to epithelial stem cells. Recent stud- ies reported that the combination of a ROCK inhibitor and a TGF-$\beta$ inhibitor enabled expansion of epithelial stem cells,[46] and Y27632 itself allowed extended passage of pluripotent stem cell-derived RPE cells and inhibited EMT through vari- ous pathways,[29] including the ROCK pathway,[33] which is involved in cytoskeleton reorganization and actin stress fiber formation.[31,32] Therefore RY treatment may also function by promoting RPE stem cell proliferation to reverse EMT in the RPE cell population. When the above observations were tested in an in vivo system, a dispase-induced reti- nal disorder model was used. Dispase, a nonspecific neutral metalloproteinase, disrupts cell-cell contact, and injection of dispase into the subretinal space or the vitreous cavity was proven to induce a PVR-like condition in rabbits and

mice,[22,35] so it was used in this study to mimic the pathological conditions of proliferative retinal diseases. As we expected, in dispase-treated rats, the RPE cells underwent EMT with abnormal localization of ZO-1 and increased expression of $\alpha$-SMA, accompanied by a reduction in ERG a-wave and ERG b-wave amplitude (Fig. 6). Again, only the combination of RepSox and Y27632 was able to attenuate the pathological changes resulting from dispase treatment, and neither RepSox nor Y27632 alone achieved meaningful improvement.

Proliferation is a hallmark of EMT in PVR. Therefore, theoretically, inhibition of EMT should inhibit proliferation. However, RY treatment increased RPE proliferation instead of reducing it. This result seemed contradictory. Then, we examined the effect of RY in promoting proliferation in high cell density cultures. We found that the number of cells in S phase in the 50% confluency condition was increased by only 55.86% after RY treatment (Supplementary Fig. S5), whereas that in the 12.5% confluency condition was increased by 141.08% after RY treatment (Figs. 5a and 5b). These results demonstrated that the effect of RY on 50% confluent cells was weaker than that on 12.5% confluent cells. Therefore we believe that RY helps RPE cells quickly establish cell-cell contact by promoting cell proliferation to avoid EMT. As the number of cells increased, the effect of RY weakened. In addition, the pathology of PVR involved the proliferation of RPE with EMT. We think RY has two roles in inhibiting PVR. First, RY inhibits EMT, and second, RY promotes RPE cell proliferation and establishment of cell-cell junctions. As soon as RPE cell-cell contact was established, the proliferation-promoting effect of RY disappeared because normal RPE cells stopped growing because of contact inhibition.

Multiple signaling pathways are involved in EMT of RPE cells, including WNT/b-catenin. Activation of WNT/b-catenin signaling mediated RPE regeneration[47] and induced EMT in ARPE-19 cells on loss of contact inhibition.[48] In this study, we also found nuclear accumulation of b-catenin in RPE cells cultured at low cell density (data not shown), indicating that b-catenin was also involved in the low-cell density–induced EMT model. We speculate that inhibition of b-catenin may also play a role in reversing low-cell density-induced EMT. The crosstalk among TGF-$\beta$, ROCK and WNT/b-catenin merits further study.

In conclusion, both the low-density, longer culture-induced EMT of RPE cells and the dispase-induced EMT of RPE cells in rats were used as models to explore the effects of some regulatory signaling molecules on the EMT process. It was clear that after EMT occurred, some molecules could intervene in the EMT process in the early state, but only the combination of RepSox and Y27632 (RY treatment) could reverse EMT in RPE cells in both the cell model and the rat model. RY treatment promoted MET, the inverse process of EMT, and maintained the function of RPE cells. The mechanism of RY treatment involved the superposition of the roles of RepSox and Y27632 by simultaneously inhibiting both the ROCK pathway and the TGF-$\beta$ pathway. This combined RY therapy may have a potential beneficial effect in proliferative retinal diseases, especially those involving EMT of RPE cells. Because proliferative retinal diseases such as PVR are highly recurrent after surgery, the most commonly used clinical treatment, our study may supply a promising strategy for millions of patients suffering from these diseases. Of course, more comprehensive basic and clinical trials are needed.

## References

1. Strauss O. The retinal pigment epithelium in visual function. *Physiol Rev*. 2005;85:845–881.

2. Grigoryan EN, Markitantova YV. Cellular and molecular preconditions for retinal pigment epithelium (RPE) natural reprogramming during retinal regeneration in urodela. *Biomedicines*. 2016;4(4):28.

3. Islam MR, Nakamura K, Casco-Robles MM, Kunahong A, Inami W, Toyama F, et al. The newt reprograms mature RPE cells into a unique multipotent state for retinal regeneration. *Sci Rep*. 2014;4:6043.

4. Kim IK, Arroyo JG. Mechanisms in proliferative vitreoretinopathy. *Ophthalmol Clin North Am*. 2002;15(1):81–86.

5. Pastor JC, de la Rua ER, Martin F. Proliferative vitreoretinopathy: risk factors and pathobiology. *Prog Retin Eye Res*. 2002;21:127–144.

6. Tamiya S, Kaplan HJ. Role of epithelial-mesenchymal transition in proliferative vitreoretinopathy. *Exp Eye Res*. 2016;142:26–31.

7. Yang S, Li H, Li M, Wang F. Mechanisms of epithelial-mesenchymal transition in proliferative vitreoretinopathy. *Discov Med*. 2015;20(110):207–217.

8. Lee SC, Kwon OW, Seong GJ, Kim SH, Ahn JE, Kay ED. Epitheliomesenchymal transdifferentiation of cultured RPE cells. *Ophthalmic Res*. 2001;33(2):80–86.

9. Tamiya S, Liu L, Kaplan HJ. Epithelial-mesenchymal transition and proliferation of retinal pigment epithelial cells initiated upon loss of cell-cell contact. *Invest Ophthalmol Vis Sci*. 2010;51:2755–2763.

10. Masszi A, Fan L, Rosivall L, et al. Integrity of cell-cell contacts is a critical regulator of TGF-beta 1-induced epithelial-to-myofibroblast transition: role for beta-catenin. *Am J Pathol*. 2004;165:1955–1967.

11. Fan L, Sebe A, Peterfi Z, et al. Cell contact-dependent regulation of epithelial-myofibroblast transition via the rho-rho kinase-phospho-myosin pathway. *Mol Biol Cell*. 2007;18:1083–1097.

12. Gasior K, Wagner NJ, Cores J, et al. The role of cellular contact and TGF-beta signaling in the activation of the epithelial mesenchymal transition (EMT). *Cell Adh Migr*. 2019;13(1):63–75.

13. O'Connor JW, Mistry K, Detweiler D, Wang C, Gomez EW. Cell-cell contact and matrix adhesion promote alphaSMA expression during TGFbeta1-induced epithelial-myofibroblast transition via Notch and MRTF-A. *Sci Rep*. 2016;6:26226.

14. Huang RY, Wong MK, Tan TZ, et al. An EMT spectrum defines an anoikis-resistant and spheroidogenic intermediate mesenchymal state that is sensitive to e-cadherin restoration by a src-kinase inhibitor, saracatinib (AZD0530). *Cell Death Dis*. 2013;4:e915.

15. Vultur A, Buettner R, Kowolik C, et al. SKI-606 (bosutinib), a novel Src kinase inhibitor, suppresses migration and invasion of human breast cancer cells. *Mol Cancer Ther*. 2008;7:1185–1194.

16. Kim LC, Song L, Haura EB. Src kinases as therapeutic targets for cancer. *Nat Rev Clin Oncol*. 2009;6:587–595.

17. Puls LN, Eadens M, Messersmith W. Current status of SRC inhibitors in solid tumor malignancies. *Oncologist*. 2011;16:566–578.

18. He H, Kuriyan AE, Su CW, et al. Inhibition of proliferation and epithelial mesenchymal transition in retinal pigment epithelial cells by heavy chain-hyaluronan/pentraxin 3. *Sci Rep*. 2017;7:43736.

19. Itoh Y, Kimoto K, Imaizumi M, Nakatsuka K. Inhibition of RhoA/Rho-kinase pathway suppresses the expression of type I collagen induced by TGF-beta2 in human retinal pigment epithelial cells. *Exp Eye Res*. 2007;84:464–472.

20. Nieto MA, Huang RY, Jackson RA, Thiery JP. Emt: 2016. *Cell*. 2016;166:21–45.

21. Radeke MJ, Radeke CM, Shih YH, et al. Restoration of mesenchymal retinal pigmented epithelial cells by TGFbeta pathway inhibitors: implications for age-related macular degeneration. *Genome Med*. 2015;7:58.

22. Frenzel EM, Neely KA, Walsh AW, Cameron JD, Gregerson DS. A new model of proliferative vitreoretinopathy. *Invest Ophthalmol Vis Sci*. 1998;39:2157–2164.

23. Zhang J, Xu G, Zhang L, et al. A modified histoimmunochemistry-assisted method for in situ RPE evaluation. *Front Biosci (Elite Ed)*. 2012;4:1571–1581.

24. Fernandez-Godino R, Garland DL, Pierce EA. Isolation, culture and characterization of primary mouse RPE cells. *Nat Protoc*. 2016;11:1206–1218.

25. Sonoda S, Spee C, Barron E, Ryan SJ, Kannan R, Hinton DR. A protocol for the culture and differentiation of highly polarized human retinal pigment epithelial cells. *Nat Protoc*. 2009;4:662–673.

26. Li P, Tian H, Li Z, Wang L, Gao F, Ou Q, et al. Subpopulations of bone marrow mesenchymal stem cells exhibit differential effects in delaying retinal degeneration. *Curr Mol Med*. 2016;16:567–581.

27. Wang L, Li P, Tian Y, et al. Human umbilical cord mesenchymal stem cells: subpopulations and their difference in cell biology and effects on retinal degeneration in RCS rats. *Curr Mol Med*. 2017;17:421–435.

28. Grisanti S, Guidry C. Transdifferentiation of retinal pigment epithelial cells from epithelial to mesenchymal phenotype. *Invest Ophthalmol Vis Sci*. 1995;36:391–405.

29. Croze RH, Buchholz DE, Radeke MJ, Thi WJ, Hu Q, Coffey PJ, et al. ROCK inhibition extends passage of pluripotent stem cell-derived retinal pigmented epithelium. *Stem Cells Transl Med*. 2014;3:1066–1078.

30. Korol A, Taiyab A, West-Mays JA. RhoA/ROCK signaling regulates TGFbeta-induced epithelial-mesenchymal transition of lens epithelial cells through MRTF-A. *Mol Med*. 2016;22:713–723.

31. Leung T, Chen XQ, Manser E, Lim L. The p160 RhoA-binding kinase ROK alpha is a member of a kinase family and is involved in the reorganization of the cytoskeleton. *Mol Cell Biol*. 1996;16:5313–5327.

32. Somlyo AP, Somlyo AV. Signal transduction by G-proteins, rho-kinase and protein phosphatase to smooth muscle and non-muscle myosin II. *J Physiol*. 2000;522(Pt 2):177–185.

33. Uehata M, Ishizaki T, Satoh H, et al. Calcium sensitization of smooth muscle mediated by a Rho-associated protein kinase in hypertension. *Nature*. 1997;389(6654):990–994.

34. Wu Q, Ouyang C, Xie L, Ling Y, Huang T. The ROCK inhibitor, thiazovivin, inhibits human corneal endothelial-tomesenchymal transition/epithelialtomesenchymal transition and increases ionic transporter expression. *Int J Mol Med*. 2017;40:1009–1018.

35. Canto Soler MV, Gallo JE, Dodds RA, Suburo AM. A mouse model of proliferative vitreoretinopathy induced by dispase. *Exp Eye Res*. 2002;75:491–504.

36. Kawka E, Witowski J, Sandoval P, et al. Epithelial-to-mesenchymal transition and migration of human peritoneal mesothelial cells undergoing senescence. *Perit Dial Int*. 2019;39:35–41.

37. Yi Y, Xie H, Xiao X, et al. Ultraviolet A irradiation induces senescence in human dermal fibroblasts by down-regulating DNMT1 via ZEB1. *Aging*. 2018;10:212–228.

38. Hay ED. An overview of epithelio-mesenchymal transformation. *Acta Anat (Basel)*. 1995;154:8–20.

39. Hannon GJ, Beach D. p15INK4B is a potential effector of TGF-beta-induced cell cycle arrest. *Nature*. 1994;371(6494):257–261.

40. Pillaire MJ, Casagrande F, Malecaze F, Manenti S, Darbon JM. Regulation by transforming growth factor-beta 1 of G1 cyclin-dependent kinases in human retinal epithelial cells. *Exp Eye Res*. 1999;68:193–199.

41. Croze RH, Thi WJ, Clegg DO. ROCK inhibition promotes attachment, proliferation, and wound closure in human embryonic stem cell-derived retinal pigmented epithelium. *Transl Vis Sci Technol*. 2016;5(6):7.

42. Kamao H, Miki A, Kiryu J. ROCK inhibitor-induced promotion of retinal pigment epithelial cell motility during wound healing. *J Ophthalmol*. 2019;2019:9428738.

43. Zhao XX, An XL, Zhu XC, et al. Inhibiting transforming growth factor-beta signaling regulates in vitro maintenance and differentiation of bovine bone marrow mesenchymal stem cells. *J Exp Zool B Mol Dev Evol*. 2018;330:406–416.

44. Liu X, Sun H, Qi J, et al. Sequential introduction of reprogramming factors reveals a time-sensitive requirement for individual factors and a sequential EMT-MET mechanism for optimal reprogramming. *Nat Cell Biol*. 2013;15:829–838.

45. Shen J, He J, Wang F. Isolation and culture of primary mouse retinal pigment epithelial (RPE) cells with rho-kinase and TGFbetaR-1/ALK5 inhibitor. *Med Sci Monit*. 2017;23:6132–6136.

46. Zhang C, Lee HJ, Shrivastava A, et al. Long-term in vitro expansion of epithelial stem cells enabled by pharmacological inhibition of PAK1-ROCK-myosin II and TGF-beta signaling. *Cell Rep*. 2018;25:598–610.e5.

47. Han JW, Lyu J, Park YJ, Jang SY, Park TK. Wnt/β-catenin signaling mediates regeneration of retinal pigment epithelium after laser photocoagulation in mouse eye. *Invest Ophthalmol Vis Sci*. 2015;56:8314–8324.

48. Chen HC, Zhu YT, Chen SY, Tseng SC. Wnt signaling induces epithelial-mesenchymal transition with proliferation in ARPE-19 cells upon loss of contact inhibition. *Lab Invest*. 2012;92:676–687.